

# INFLUENCE OF SOFTENING ROCK MASS BEHAVIOR IN 3D SIMULATIONS OF DEEP TUNNELING

MAGDALENA SCHRETER<sup>†,\*</sup>, MATTHIAS NEUNER\*, PETER GAMNITZER\* AND  
GÜNTER HOFSTETTER\*

\*University of Innsbruck  
Innsbruck, AUSTRIA

<sup>†</sup>e-mail: [magdalena.schreter@uibk.ac.at](mailto:magdalena.schreter@uibk.ac.at)

**Key words:** Rock Mass, Deep Tunneling, Damage-Plasticity Model, Hoek-Brown failure criterion

**Abstract.** The present contribution is concerned with finite element modeling of NATM tunneling with special emphasis on adequately modeling the highly nonlinear mechanical behavior of rock mass up to failure. Based on a numerical study of deep tunneling, derived from a stretch of the Brenner Base Tunnel, the mechanical behavior predicted by the novel gradient-enhanced rock damage-plasticity model will be assessed in large-scale, three-dimensional finite element simulations and compared with the one on the basis of a commonly employed linear elastic-perfectly plastic rock model. A significant difference in the mechanical response of the tunnel structure is obtained: employing the rock damage-plasticity model reveals a substantial increase of the displacements in the vicinity of the tunnel due to softening rock mass behavior. Consequently, higher loads are imposed onto the tunnel support, increasing the required load-bearing capacity.

## 1 INTRODUCTION

In addition to monitoring and exploration instruments, finite element simulations are valuable tools for analyzing the complex mechanical behavior of the rock-support system during tunneling. The latter serve for (i) predicting the deformations during the construction process, (ii) dimensioning of the tunnel support and (iii) recognizing potentially dangerous situations related to collapse of the tunnel structure. Nevertheless, their predictive power depends strongly on the employed constitutive models for the interacting materials such as the surrounding rock mass and the tunnel support consisting of, e.g., shotcrete shells.

A commonly employed construction method for tunnels with high overburden in rock mass is the New Austrian Tunneling Method (NATM), which is flexibly adaptable to the prevailing conditions. Therein, the major construction

principle is to utilize the strength of the surrounding rock mass as the major load-bearing part. During the construction of deep tunnels the high primary stresses prevailing in the rock mass are heavily redistributed, which may lead to structural changes and crack formation in the rock mass. The latter have substantial impact on the mechanical behavior of the tunnel structure, leading in the worst case even to collapse.

For describing the mechanical rock mass behavior in simulations of tunneling, linear elastic-perfectly plastic constitutive models with Hoek-Brown or Mohr-Coulomb type failure criterion are frequently used [1]. However, these simplified models neglect the important mechanical effects of strain hardening as well as strain softening accompanied by stiffness degradation, which are observed in stress-strain curves of rock specimens. Especially the latter effects play a key role when the stability

of the rock-support system is analyzed during tunnel advance.

Thus, aiming at an adequate representation of the nonlinear stress-strain behavior of rock in the pre-peak and the post-peak regime of the stress-strain relation, an isotropic rock damage-plasticity (RDP) model was proposed in [2], extended by a gradient-enhanced damage formulation in [3]. The performance of the RDP model was assessed in [4] based on simplified two-dimensional finite element simulations of deep NATM tunneling. Therein, softening in the rock mass manifested in localization of deformation into narrow zones of distinct shear bands in the vicinity of the tunnel. In these simplified two-dimensional simulations, several assumptions are necessary to account for the influence of the tunneling process on the analyzed cross section. Furthermore, three-dimensional mechanical effects such as horizontal deformations of the tunnel face cannot be analyzed.

In the present contribution, the numerical investigation on the highly nonlinear mechanical behavior of rock mass including softening behavior in deep tunneling is continued. For this purpose, a large-scale three-dimensional finite element model is developed, derived from a stretch of the Brenner Base Tunnel constructed by the NATM in Innsbruck quartz phyllite rock mass. In contrast to the previous two-dimensional study [4], the influence of three-dimensional effects can be assessed and the real drill, blast and secure construction process is modeled in a natural way. Nevertheless, such a large-scale simulation poses a demanding computational effort. The mechanical behavior of the rock-support system is assessed by employing two types of constitutive rock models: (i) a linear elastic-perfectly plastic rock model, as a representative for commonly employed rock models, and (ii) the gradient-enhanced RDP model.

## 2 CONSTITUTIVE ROCK MODELS

In the following, two constitutive models for rock mass, (i) the linear elastic-perfectly plastic Hoek-Brown model and (ii) the gradient-

enhanced rock damage-plasticity model are described briefly. Both models assume isotropic material behavior of rock mass. Furthermore, rock mass consisting of intact rock and discontinuities is treated as an equivalent continuum. For estimating the equivalent mechanical properties of rock mass, empirical reduction factors to account for the influence of discontinuities proposed by [5, 6] are employed. They are calculated by means of two geological parameters, the geological strength index  $GSI$  and the disturbance factor  $D$ .

Since both constitutive models are highly nonlinear, for improving the numerical stability of the solution procedure, a visco-plastic Duvaut-Lions type formulation [7] is considered. Therein, a small relaxation time ( $10^{-7}$  h) acts as a numerical stabilization parameter without significantly influencing the results.

### 2.1 Hoek-Brown Model

As a representative model for established models in engineering practice, a linear elastic-perfectly plastic model is chosen, denoted as Hoek-Brown model. In this model, the well-known failure criterion by Hoek and Brown [8] in the smooth version by Menétrey and Willam [9] is employed. For the evolution of plastic strain, a Mohr-Coulomb type plastic potential function is chosen, yielding a non-associated flow rule. The parameters for intact rock of the Hoek-Brown model comprise Young's modulus  $E$ , Poisson's ratio  $\nu$ , the friction parameter  $m_0$  and the dilation angle  $\psi$ .

### 2.2 Gradient-Enhanced Rock Damage-Plasticity Model

The rock damage-plasticity (RDP) model was presented in [2, 10]. For obtaining mesh-independent results in the softening regime, the implicit gradient-enhanced extension of the damage formulation of the RDP model was proposed in [3], where a detailed model description is provided for the interested reader.

For modeling the highly nonlinear stress-strain behavior of rock, linear elasticity, non-associated plasticity, nonlinear isotropic strain

hardening and strain softening are considered in the RDP model. It is formulated based on the coupling of the flow theory of plasticity and the theory of continuum damage mechanics. The total stress-strain relation is expressed as

$$\boldsymbol{\sigma} = (1 - \omega) \mathbb{C} : (\boldsymbol{\varepsilon} - \boldsymbol{\varepsilon}^p) = (1 - \omega) \bar{\boldsymbol{\sigma}}, \quad (1)$$

in which  $\boldsymbol{\sigma}$  denotes the nominal Cauchy stress tensor,  $\mathbb{C}$  the fourth-order elastic stiffness tensor,  $\boldsymbol{\varepsilon}$  the total strain tensor and  $\boldsymbol{\varepsilon}^p$  the plastic strain tensor. The nominal stress tensor  $\boldsymbol{\sigma}$  (force per total area) is linked to the effective stress tensor  $\bar{\boldsymbol{\sigma}}$  (force per undamaged area) by the scalar isotropic damage parameter  $\omega$ , ranging from 0 (undamaged material) to 1 (fully damaged material).

The implicit gradient-enhanced damage formulation introduces nonlocality into the damage formulation of the RDP model. To this end, in addition to the local strain-like softening variable  $\alpha_d$ , which originally governs the evolution of the damage parameter  $\omega(\alpha_d)$ , a nonlocal softening variable  $\bar{\alpha}_d$  is introduced, leading to a modified damage law  $\omega(\bar{\alpha}_d, \alpha_d)$  for the gradient-enhanced RDP model. Following the implicit-gradient enhanced framework proposed by [11], the nonlocal softening variable is implicitly defined by an additional partial differential equation of Screened-Poisson's type

$$\bar{\alpha}_d - l^2 \Delta \bar{\alpha}_d = \alpha_d \quad \text{in } \Omega \quad (2)$$

with the length parameter  $l$  representing the zone of nonlocal interaction. By calculating a weighted average of the local and nonlocal softening variable by means of

$$\hat{\alpha}_d(\alpha_d, \bar{\alpha}_d) = m \bar{\alpha}_d + (1 - m) \alpha_d \quad (3)$$

with the weighting parameter  $m$ , the modified damage law

$$\omega(\bar{\alpha}_d, \alpha_d) = 1 - \exp(-\hat{\alpha}_d(\bar{\alpha}_d, \alpha_d)/\varepsilon_f) \quad (4)$$

of the gradient-enhanced RDP model is obtained. Choosing the weighting parameter  $m > 1$  resembles the over-nonlocal formulation as

suggested by [12] for full regularization. Considering (2) together with the standard equilibrium equation yields a fully coupled set of PDE for the unknown displacement field  $\boldsymbol{u}$  and the nonlocal softening variable  $\bar{\alpha}_d$ . It was demonstrated in [3] that by employing the gradient-enhanced RDP model mesh-independent results are obtained, even for complex damage patterns like shear bands around a tunnel.

The parameters of the gradient-enhanced RDP model for intact rock comprise Young's modulus  $E$ , Poisson's ratio  $\nu$ , the friction parameter  $m_0$ , the uniaxial compressive yield strength  $f_{cy}$ , the dilatancy parameter  $m_{gl}$ , two hardening parameters  $A_h$  and  $C_h$ , the softening parameter  $A_s$ , the softening modulus  $\varepsilon_f$ , the nonlocal radius  $l$  and the weighting parameter  $m$ .

### 2.3 Material Parameters of Innsbruck Quartz Phyllite

The parameters for intact rock of Innsbruck quartz phyllite for the Hoek-Brown model and for the gradient-enhanced RDP model were determined from a best fit with the experimental results of triaxial compression tests on Innsbruck quartz phyllite specimens [4, 13]. For calculating the empirical reduction factors for the transition from intact rock to rock mass, the geological strength index  $GSI$  and the disturbance factor  $D$  were specified according to the geological survey as 50 and 0, respectively. Accordingly, the material parameters of Innsbruck quartz phyllite are summarized in Table 1 for the Hoek-Brown model and in Table 2 for the gradient-enhanced RDP model.

Table 1: Material parameters for the Hoek-Brown model representing intact Innsbruck quartz phyllite.

$E$ (MPa)	$\nu$ (-)	$f_{cu}$ (MPa)	$m_0$ (-)	$\psi$ (-)
56 670	0.2	41.6	12.0	12°

Table 2: Material parameters for the gradient-enhanced RDP model representing intact Innsbruck quartz phyllite.

$E$ (MPa)	$\nu$ (-)	$f_{cu}$ (MPa)	$m_0$ (-)	$f_{cy}$ (MPa)	$m_{g1}$ (-)
56 670	0.2	41.6	12.0	29.5	9
$A_h$ (-)	$C_h$ (-)	$A_s$ (-)	$\varepsilon_f$ (-)	$l$ (mm)	$m$ (-)
0.0045	8.8	40.0	$1.2 \times 10^{-3}$	100	1.05

### 3 3D FINITE ELEMENT MODEL OF DEEP TUNNELING

The gradient-enhanced RDP model model is employed in large-scale, three-dimensional finite element simulations of deep tunneling and its influence on the mechanical behavior is assessed and compared with the one on the basis of the Hoek-Brown model. To this end, in a numerical study, the construction of a stretch of the Brenner Base Tunnel with 950 m overburden in Innsbruck quartz phyllite rock mass by means of a drill, blast and secure procedure is considered. The excavation sequence was split into top heading-bench and invert. The installed tunnel support consisted of a 20 cm thick shotcrete shell, 4 m long rock bolts and lattice girders. During the construction process comprehensive in-situ measurements were performed over a tunnel length of 40 m, reported in [14, 15]. Two inclinometer chains were placed approximately 1 m above the crown, recording vertical displacements in the rock mass even prior to the passage of the tunnel face.

A large-scale three-dimensional finite element model of the tunnel stretch of interest, accounting for the real excavation and securing process, is developed. The finite element simulations are performed on a high performance computer, using the OpenMPI parallelized C++ framework by [16] with an iterative solver (block-preconditioned GMRES).

The initial boundary value problem is illustrated in Figure 1. A tunnel stretch of 20 m with a tunnel diameter of 8.5 m is analyzed, mak-

ing a compromise between efficiency by limiting the problem size and accuracy by achieving the central model part being unaffected by the external model boundaries.

The initial geostatic stress field is assumed depth-dependent with a gravity-induced stress gradient ( $\gamma = 27 \text{ kN/m}^3$ ) and a lateral stress coefficient of 0.8, yielding initial normal stress components of  $\sigma_y = -25.6 \text{ MPa}$ ,  $\sigma_x = -20.5 \text{ MPa}$  and  $\sigma_z = -20.5 \text{ MPa}$  at the tunnel axis. Perpendicular to the model boundaries, homogeneous Dirichlet boundary conditions for the displacement field and homogeneous Neumann boundary conditions for the nonlocal softening field are assumed.

Perpendicular to the tunnel axis, a  $50 \text{ m} \times 100 \text{ m}$  domain of rock mass is modeled, assuming symmetry conditions with respect to the  $xy$ -plane. The rock mass is discretized using 20-node hexahedral continuum elements with reduced integration. Both the displacement field and the field of the nonlocal softening variable are interpolated by quadratic functions. In the vicinity of the tunnel the distance between two adjacent nodes is approximately 0.1 m, corresponding to the employed length parameter of the gradient-enhanced rock damage-plasticity model.

To trigger the damage-induced strain localization in the rock mass, non-uniformly distributed rock mass properties are assumed by introducing zones in which the strength of the rock mass is slightly weakened (indicated by light-brown areas in Figure 1(b)). It was verified that these weakened zones do not affect the predicted mechanical response prior to the onset of strain softening in the rock mass [4].

For the tunnel support, a shotcrete shell and rock bolts are considered. The shotcrete shell is modeled by the same type of finite elements considering 4 elements across the thickness with linear elastic material behavior ( $E = 7000 \text{ MPa}$ ,  $\nu = 0.21$ ). The rock bolts (6 per tunnel side, cross-sectional area  $4.9 \text{ cm}^2$ ) are modeled by 2-node truss elements embedded perfectly bonded in the rock elements and with perfect von Mises plasticity ( $E = 210\,000 \text{ MPa}$ ,

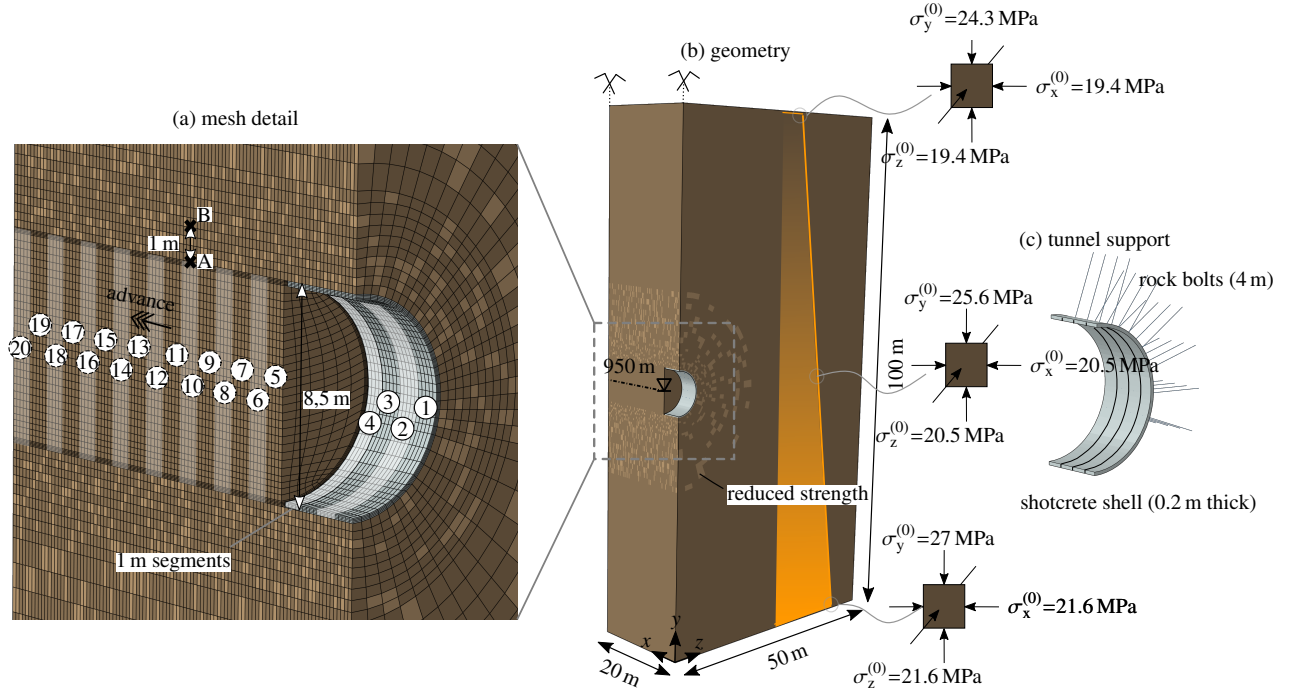


Figure 1: 3D initial boundary value problem of deep tunneling.

$\nu = 0.15$ ,  $f_{cy} = 550$  MPa). Accordingly, the discretized 3D model consists of 117500 rock elements, 14400 shotcrete elements and 3360 truss elements.

The excavation of the circular profile is simplified, considering full-face excavation. Working cycles of 8 h are modeled, in which after blasting of a 1 m tunnel segment within 0.1 h securing of the segment by placing a 0.2 m thick shotcrete shell and rock bolts of 4 m length is realized. As an example, Figure 1(a) illustrates the construction stage after placement of the 4th shotcrete segment. It should be noted that time-dependent material behavior is not considered, only visco-plasticity for numerical stabilization.

For the present numerical study, the predicted mechanical behavior of the rock-support system is assessed, considering two different simulations:

- *Sim. 1*: The complete rock mass is modeled by the Hoek-Brown model.
- *Sim. 2*: The rock mass to be excavated is modeled by the Hoek-Brown model to circumvent the loss of stability of the tunnel face already during the first construc-

tion stages. In the near field of the tunnel the gradient-enhanced RDP model is employed.

## 4 RESULTS

The influence of softening rock mass behavior on the predicted mechanical behavior of the tunnel structure is assessed by comparing the numerical results of Sim. 2 to Sim. 1 in terms of (i) the evolution of displacements, (ii) the stress in the surrounding rock mass and (iii) the stress in the shotcrete shell, indicating the loading of the tunnel structure.

### 4.1 Displacements

Figure 2 illustrates the distribution of the displacement magnitude of the deformed tunnel structure predicted by Sim. 1 (a-b) and Sim. 2 (c-d). In these figures, two different tunneling stages are considered: after construction of the 5th segment ( $t = 40$  h) and the 11th segment ( $t = 80$  h). In both simulations, the influence of the external boundary on the displacement distribution for the first segments is clearly visible by larger displacement magnitudes. In Sim. 1, the largest displacement magnitude of 17 mm evolves at the tunnel face. The displacement

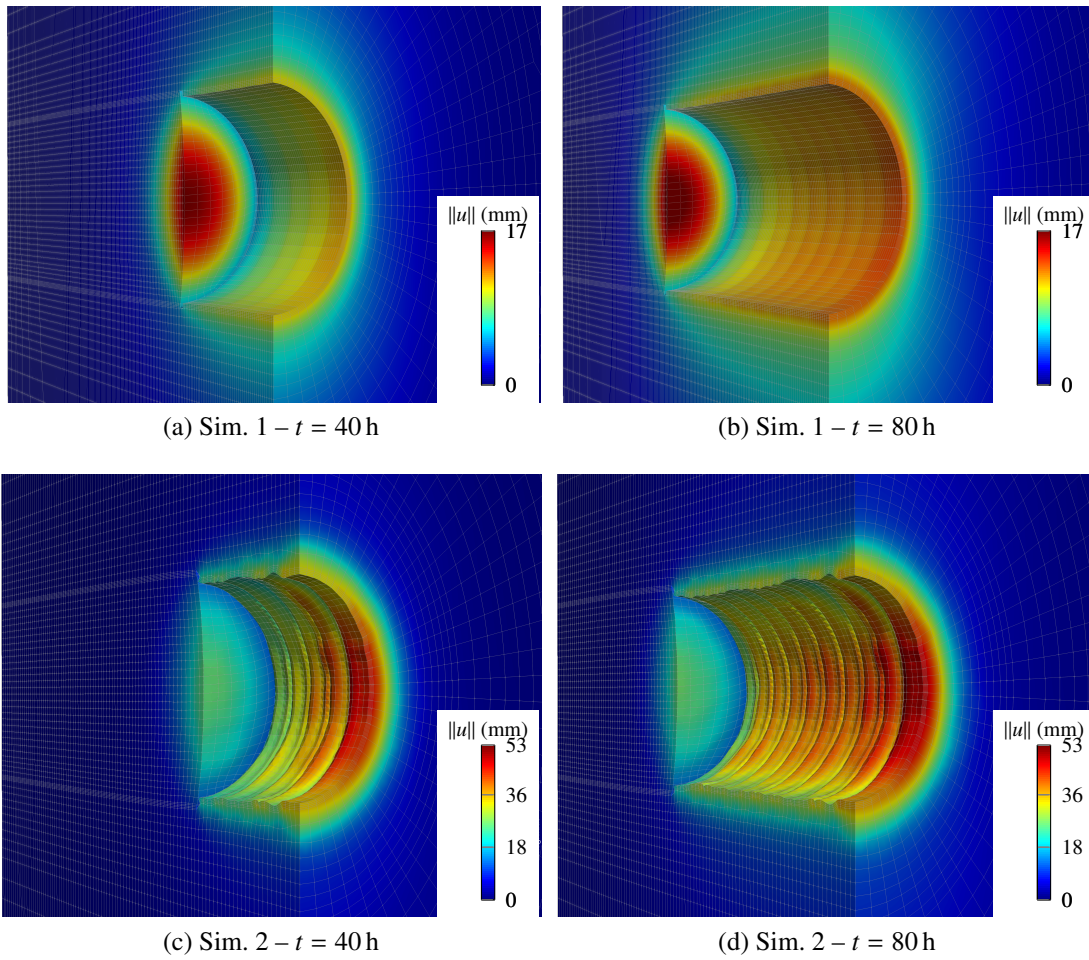


Figure 2: Distribution of the displacement magnitude in the deformed rock-support system (magnification factor of 20) predicted by the Hoek-Brown model (a-b) and the RDP model (c-d), after placement of the tunnel support.

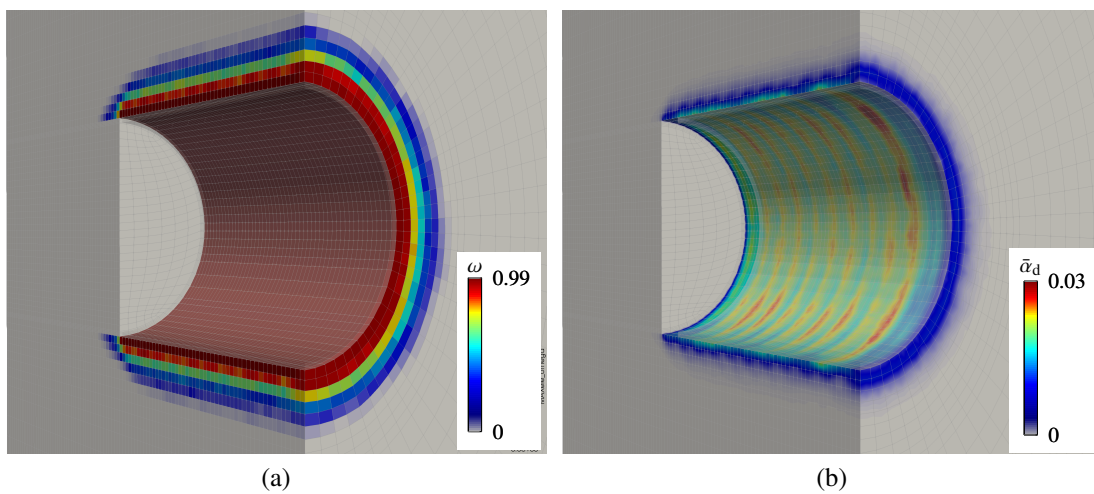


Figure 3: Distribution of the damage variable (a) and the nonlocal softening variable (b) in the rock mass in Sim. 2 at  $t = 80$  h, after placement of the tunnel support.

magnitude within individual segments is almost uniform along the perimeter although a reduced lateral stress coefficient of the geostatic stress state is assumed. With progressing tunnel advance, it can be seen that beyond the reduced influence through the tunnel face a steady distribution of the displacement magnitude is obtained, visible in Figure 2(b).

In Sim. 2, the maximum displacement magnitude of 53 mm is predicted along the tunnel side walls (cf. Figure 2(c-d)). Furthermore, the displacements within individual tunnel segments are not uniform but rather concentrate within the side wall of a segment. This is related to the damage evolution in the rock mass in the vicinity of the tunnel, indicated in Figure 3(a), where the rock elements adjacent to the shotcrete shell are completely damaged. The slightly non-uniformly distributed material properties in the surrounding rock mass result only in a slight fluctuation of the damage variable. In Figure 3(b) the corresponding distribution of the nonlocal softening variable, which can be interpreted as an equivalent plastic strain, is illustrated. The nonlocal softening variable concentrates in rings along the tunnel perimeter. For a better resolution of the nonlocal softening variable, a finer mesh could be chosen, at the expense of an increasing computational cost. It is concluded that localization of deformation is obtained in the longitudinal direction while in perpendicular planes the displacement distribution is smooth. This is in contrast to the previous 2D simulations [4] of a single cross section, where localization of deformation into distinct shear bands in the plane perpendicular to the tunnel axis was predicted.

Figures 4 and 5 illustrate the temporal evolution of the vertical displacement of Point A and Point B, respectively, obtained by Sim. 1 and Sim. 2. Both points are located at the 11th segment, depicted in Figure 1(a). The gray shaded area indicates the time range until the tunnel face reaches the points A and B. In both graphs, the segment-by-segment excavation and securing tunneling procedure is reflected in the step-wise increase of displace-

ments, yielding the largest incremental increase of displacements during excavation of the corresponding 11th segment at 80 h.

During excavation of this segment, at Point A (cf. Figure 4) in Sim. 1 the vertical displacement magnitude increases from 4 mm to 7 mm. In Sim. 2 due to accumulation of severe damage in the rock mass at this point (cf. Figure 3(a)) a substantial larger increase of displacements from 7 mm to 20 mm is obtained. After completion of the tunnel at 160 h, striking discrepancies in the predicted displacements are recognized: in Sim. 1 a vertical displacement magnitude of 13 mm is obtained compared to 30 mm in Sim. 2.

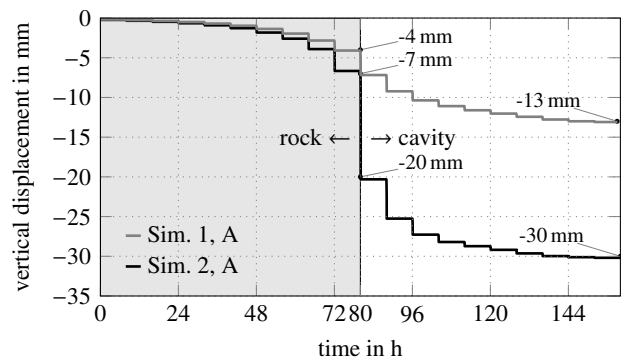


Figure 4: Temporal displacement evolution, evaluated at Point A (cf. Figure 1(a)).

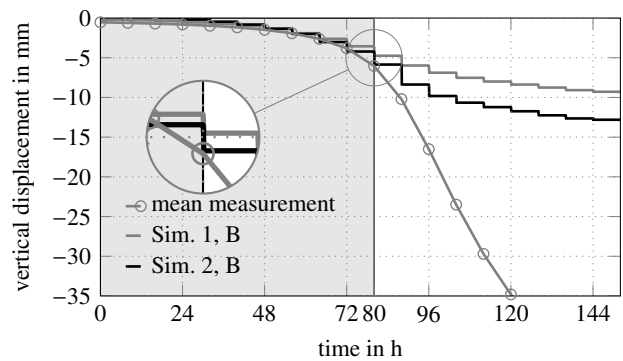


Figure 5: Temporal displacement evolution, evaluated at Point B (cf. Figure 1(a)).

The predicted vertical displacement magnitudes at Point B (1 m above Point A), illustrated in Figure 5, are considerably smaller compared to Point A, since Point B is affected by a lower degree of damage (cf. Figure 3(a)). In addition to the numerically predicted displacements, the

recorded mean value of the vertical displacement measured by the inclinometer chains [15] is depicted. Prior to the arrival of the tunnel face, the numerically obtained displacements at the corresponding Point B are in excellent agreement with the measurement data. Subsequently, the measured displacements are significantly larger than the numerical ones. However, faulty measurement data is suspected due to exposure of several blasts and potential damage of the inclinometers [15].

## 4.2 Circumferential Stress

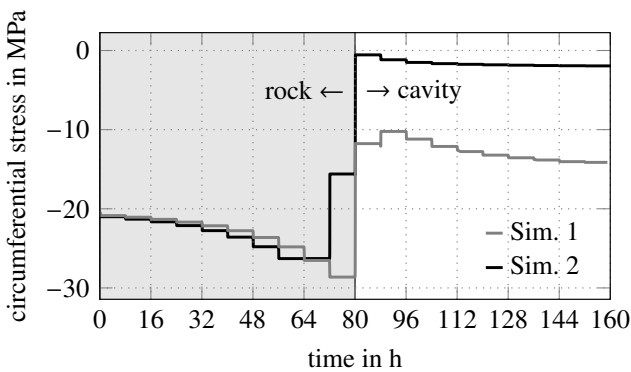


Figure 6: Evolution of the circumferential stress in the rock mass, evaluated at the rock element adjacent to Point A (cf. Figure 1(a)).

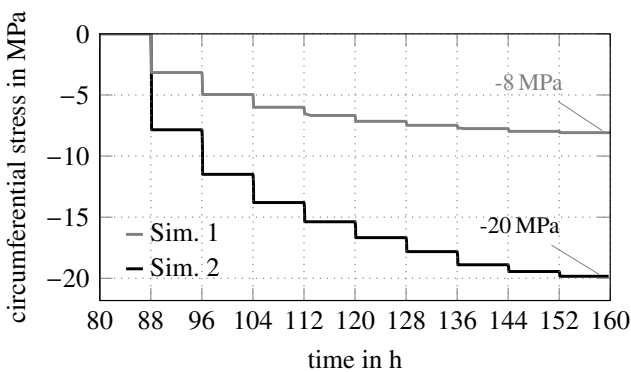


Figure 7: Evolution of the circumferential stress in the shotcrete shell, evaluated at the shotcrete element adjacent to Point A (cf. Figure 1(a)).

Figure 6 depicts the temporal evolution of the circumferential stress in the rock mass, computed in the rock element adjacent to Point A. By comparison of the results of Sim. 1 and Sim. 2, prior to passage of the tunnel face

in Sim. 1 the circumferential stress magnitude is increasing continuously while in Sim. 2 the magnitude of the circumferential stress is already decreasing during construction of the previous 10th segment. This indicates that in Sim. 2 the stress redistribution in the rock mass during tunneling induces damage also in the rock mass behind the tunnel face.

Figure 7 illustrates the temporal evolution of the circumferential stress in the shotcrete shell in the shotcrete element adjacent to Point A. Initially, the shotcrete shell is placed in a stress-free state. Comparing the final circumferential stress magnitudes, the one of Sim. 2 (-20 MPa) is twice the value obtained in Sim. 1 (-8 MPa). This indicates that due to the larger imposed deformations onto the shotcrete shell in Sim. 2 the tunnel support must sustain higher loads.

## 4.3 Computational Cost

The presented simulations were performed on a distributed memory cluster consisting of Intel Xeon E5-2690 v4 CPUs, using 80 cores for the simulations. In Sim. 2 the balance of the accumulated computational effort of 248 h is composed as follows:

- 207 h for solution of the linear equation systems,
- 27 h for computation of the element stiffness matrix and the element load vector and
- 14 h for process communication, assembly of the system matrix, application of the boundary conditions and output.

Thus, the largest share of the total computation time is spent on solving the linear system of equations by the iterative solver. This is related to the large number of DOF and the obtained large number of nonzero entries per row in the stiffness matrix due to the quadratic interpolation functions of the unknown displacement and nonlocal field. Thus, for reducing the simulation time, a different solver type could be investigated.

## 5 CONCLUSIONS

Large-scale three-dimensional finite element simulations of the mechanical behavior of the rock-support system during NATM tunneling, derived from a stretch of the Brenner Base Tunnel, were performed. In contrast to commonly employed simplified 2D analyses, three-dimensional effects and the real drill, blast and secure construction process can be modeled at the expense of a substantially higher computational effort.

The focus of the investigation was on adequate modeling the highly nonlinear rock mass behavior up to failure. Based on the simulations of deep tunneling, the mechanical behavior of the rock-support system predicted by the gradient-enhanced rock damage-plasticity model [3] was assessed and compared with the one on the basis of a simpler, commonly used linear elastic-perfectly plastic rock model.

The main differences of the predicted mechanical behavior is summarized as follows: Employing the rock damage-plasticity model, the strong redistribution of the primary stress state leads to damage in the rock mass in the vicinity of the tunnel. As a consequence, larger deformations and a substantially higher loading of the shotcrete shell were obtained compared to the simulations with the linear elastic-perfectly plastic rock model. In contrast to previously performed 2D simulations in [4] using the rock damage-plasticity model, localization of deformation into distinct shear bands in cross-sectional planes was not predicted.

In the presented simulations, for the rock mass being excavated, a perfectly-plastic rock mass behavior was assumed since otherwise loss of stability of the tunnel face due to massive damage occurs already during the first construction stages. The stability of the tunnel face using the rock damage-plasticity model will be investigated separately in a forthcoming paper. Furthermore, the formation of shear bands in the vicinity of the tunnel will be studied in 3D simulations more detailed, also for comparison with the results of the previous 2D simulations [4]. Last but not least, time-dependent material

behavior of shotcrete will be considered.

## ACKNOWLEDGEMENT

The authors gratefully acknowledge partial financial support of the Brenner Base Tunnel SE. Furthermore, the authors express their sincere gratitude to Tobias Cordes from the Brenner Base Tunnel SE for providing the measurement data by the inclinometer chain. The computational results presented have been achieved in part using the HPC infrastructure LEO of the University of Innsbruck.

## REFERENCES

- [1] A Negro and P. I. B. de Queiroz. Prediction and performance: A review of numerical analyses for tunnels. In O. Kusakabe, K. Fujita, and Y. Miyazaki, editors, *Geotechnical Aspects of Underground Construction in Soft Ground*, pages 409–418, Rotterdam, The Netherlands, 2000. CRC Press Balkema.
- [2] D. Unteregger, B. Fuchs, and G. Hofstetter. A damage plasticity model for different types of intact rock. *International Journal of Rock Mechanics and Mining Sciences*, 80:402–411, 2015.
- [3] M. Schreter, M. Neuner, and G. Hofstetter. Evaluation of the implicit gradient-enhanced regularization of a damage-plasticity rock model. *Applied Sciences*, 8(6):1004, 2018.
- [4] M. Schreter, M. Neuner, D. Unteregger, and G. Hofstetter. On the importance of advanced constitutive models in finite element simulations of deep tunnel advance. *Tunnelling and Underground Space Technology*, 80:103–113, 2018.
- [5] E. Hoek, C. Carranza-Torres, and B. Corkum. Hoek-Brown failure criterion – 2002 edition. In Reginald Hammah, editor, *Proceedings of the 5th North American Rock Mechanics Symposium and the 17th Tunnelling Association*

- of Canada*, pages 267–273, Toronto, Ontario, Canada, 2002. University of Toronto Press.
- [6] E. Hoek and M. S. Diederichs. Empirical estimation of rock mass modulus. *International Journal of Rock Mechanics and Mining Sciences*, 43(2):203–215, 2006.
- [7] J. C. Simo, J. G. Kennedy, and S. Govindjee. Non-smooth multisurface plasticity and viscoplasticity – loading/unloading conditions and numerical algorithms. *International Journal for Numerical Methods in Engineering*, 26(10):2161–2185, 1988.
- [8] E. Hoek and E. T. Brown. Empirical strength criterion for rock masses. *Journal of the Geotechnical Engineering Division, Proceedings of the American Society of Civil Engineers*, 106(GT9):1013–1035, 1980.
- [9] P. Menétrey and K. J. Willam. Triaxial failure criterion for concrete and its generalization. *ACI Structural Journal*, 92(3):311–318, 1995.
- [10] D. Unteregger. *Advanced constitutive modeling of intact rock and rock mass*. PhD thesis, University of Innsbruck, 2015.
- [11] L. H. Poh and S. Swaddiwudhipong. Over-nonlocal gradient enhanced plastic-damage model for concrete. *International Journal of Solids and Structures*, 46(25-26):4369–4378, 2009.
- [12] P. A. Vermeer and R. B. J. Brinkgreve. A new effective non-local strain measure for softening plasticity. In R. Chambon, J. Desrues, and I. Vardoulakis, editors, *Localisation and Bifurcation Theory for Soils and Rocks*, pages 89–100. Society of Petroleum Engineers, CRC Press Taylor & Francis Group, 1994.
- [13] M. Schreter, M. Neuner, D. Unteregger, G. Hofstetter, C. Reinhold, T. Cordes, and K. Bergmeister. Application of a damage plasticity model for rock mass to the numerical simulation of tunneling. In G. Hofstetter, K. Bergmeister, J. Eberhardsteiner, G. Meschke, and H. F. Schweiger, editors, *Proceedings of the 4. International Conference on Computational Methods in Tunneling and Sub-surface Engineering (EURO:TUN 2017)*, pages 549–556. University of Innsbruck, Austria, 2017.
- [14] D. Unteregger. In situ Messprogramm Anfahrtsstützen EKS BBT. Technical report, University of Innsbruck, 2015. unpublished.
- [15] B. Schneider-Muntau, C. Reinhold, T. Cordes, I. Bathaeian, and K. Bergmeister. Validation of longitudinal displacement profiles by measurement at the Brenner Base Tunnel. *Geomechanics and Tunnelling*, 11(5):566–574, 2018.
- [16] P. Gamnitzer and G. Hofstetter. Fully coupled multi-phase modelling of pumping induced settlements, air-and water flow in multi-layered normally consolidated soils. *Computers and Geotechnics*, 79:10–21, 2016.